NeuroImage 103 (2014) 267–279

Contents lists available at ScienceDirect

NeuroImage

journal homepage: www.elsevier.com/locate/ynimg

Does resting-state connectivity reflect depressive rumination? A tale of two analyses

Marc G. Berman [a,*], Bratislav Misic [b], Martin Buschkuehl [c], Ethan Kross [d], Patricia J. Deldin [d], Scott Peltier [d], Nathan W. Churchill [b], Susanne M. Jaeggi [e], Vasily Vakorin [b], Anthony R. McIntosh [b], John Jonides [d]

[a] The University of Chicago, USA
[b] The Rotman Research Institute at Baycrest, Canada
[c] MIND Research Institute, Irvine, CA, USA
[d] The University of Michigan, USA
[e] The University of California at Irvine, USA

ARTICLE INFO

Article history:
Accepted 11 September 2014
Available online 26 September 2014

Keywords:
Depression
Rumination
fMRI
Functional connectivity
Multivariate analysis
Resting-state

ABSTRACT

Major Depressive Disorder (MDD) is characterized by rumination. Prior research suggests that resting-state brain activation reflects rumination when depressed individuals are not task engaged. However, no study has directly tested this. Here we investigated whether resting-state epochs differ from induced ruminative states for healthy and depressed individuals. Most previous research on resting-state networks comes from seed-based analyses with the posterior cingulate cortex (PCC). By contrast, we examined resting state connectivity by using the complete multivariate connectivity profile (i.e., connections across all brain nodes) and by comparing these results to seeded analyses. We find that unconstrained resting-state intervals differ from active rumination states in strength of connectivity and that overall connectivity was higher for healthy vs. depressed individuals. Relationships between connectivity and subjective mood (i.e., behavior) were strongly observed during induced rumination epochs. Furthermore, connectivity patterns that related to subjective mood were strikingly different for MDD and healthy control (HC) groups suggesting different mood regulation mechanisms.

Introduction

Many researchers have found differences in brain connectivity during unconstrained "resting-state" intervals between healthy persons and individuals diagnosed with Major Depressive Disorder (Berman et al., 2011; Bohr et al., 2012; Broyd et al., 2009; Greicius et al., 2007; Sheline et al., 2010; Zeng et al., 2012; Zhang et al., 2011). These differences in brain connectivity are often interpreted as being a neural mechanism reflecting depressive rumination (Berman et al., 2011; Greicius et al., 2007; Hamilton et al., 2011; Whitfield-Gabrieli and Ford, 2012), a negative repetitive thought process that characterizes depression (Nolen-Hoeksema et al., 2008; Treynor et al., 2003). No research, however, has directly tested whether the thinking during "rest" is the same as that of directly induced rumination for participants with depression compared to non-depressed participants. The first goal of the present study was to investigate whether patterns of functional connectivity during unconstrained resting-state epochs differed from active rumination in depressed and healthy individuals. Uncovering this would greatly aid our understanding of the neural processes associated with depressive rumination. To do so, we designed an experimental paradigm to assess baseline resting-states and compared those intervals to induced ruminative states and resting-states that occurred after induced rumination. The baseline resting-states were first tested so as not to be contaminated by our induced-rumination procedure.

The second goal of the present study was to investigate whether different results would be uncovered from seed-based analyses compared to analyses of the full connectivity profile (i.e., how all brain areas are connected to all other areas) for healthy controls (HCs) and individuals diagnosed with depression. There has been some debate in the literature where many studies report hyper-connectivity or hyper-activation in the default-mode network in MDD (Berman et al., 2011; Broyd et al., 2009; Greicius et al., 2007; Sheline et al., 2010), whereas other studies find decreased connectivity in MDD in a few different resting-state networks (Veer et al., 2010). Recent studies have found that the full connectivity profile was highly sensitive in discriminating healthy vs. depressed individuals at rest (Veer et al., 2010; Zeng et al., 2012). We sought to investigate whether hyper- or hypo-connectivity results depended on whether analyses were based on singular brain networks or all brain networks in their totality. To this end, we implemented a seed-based analysis with the Posterior Cingulate Cortex (PCC) to focus our analysis on a single network; the "default-mode" network and compared those results to an analysis where we explored connectivity between all brain nodes.

* Corresponding author at: Department of Psychology, The University of Chicago, 5848 South University Avenue, Chicago, IL 60637, USA. Fax: +1 773 702 0886.
E-mail address: bermanm@uchicago.edu (M.G. Berman).

http://dx.doi.org/10.1016/j.neuroimage.2014.09.027
1053-8119/

To identify global patterns of functional connectivity and how those patterns differed across groups and cognitive states (resting states and induced rumination states) we implemented a partial-least squares analysis (PLS; Krishnan et al., 2011; McIntosh and Lobaugh, 2004; McIntosh and Misic, 2013). As a multivariate statistical framework, PLS determines the combination of groups and experimental conditions that is optimally related to a spatiotemporal pattern of neural activity. We used PLS in a novel way, by entering functional connections between all possible pairs of brain regions as dependent variables, rather than activation contrasts or singular seed correlations, which are typically used. For the present study, this application of PLS offered a few important advantages. First, we were able to capture patterns of functional connections that covary together. Thus, these patterns are naturally interpretable as coherent functional networks. Second, PLS offers a framework to examine how these changes in functional connectivity were related to changes in subjective mood, which is rarely performed when examining functional connectivity. Lastly, we were able to investigate the dominant functional connectivity patterns without having to specify a priori hypotheses about the differentiation of groups and experimental conditions. Thus, we used the analysis to determine the similarities and differences between resting-states and induced rumination in a completely data-driven way.

In summary, we set out to achieve two goals in this study. The first was to examine whether resting-state epochs differed from induced rumination states for participants diagnosed with major depression compared to non-depressed controls. We assessed these potential differences both behaviorally and with multivariate measures of functional connectivity. The second goal of the study was to assess how different measures of functional connectivity, i.e. seed-based vs. global connectivity, could help to distinguish the groups during rest vs. induced rumination.

Materials and methods

Note: These fMRI parameters, task parameters and analysis parameters are similar to those from Misic et al. (in press).

Participants

Seventeen participants diagnosed with clinical depression [mean age = 26.6 years, SD = 5.94; 12 female, mean Beck Depressive Inventory (Beck et al., 1996) (BDI) = 29.8] and seventeen non-depressed controls (mean age = 24.2 years, SD = 5.95; 12 female, mean BDI = 1.4) participated in our study. Participants' diagnosis of MDD vs. a non-diagnosis was determined by a trained clinician administering the Structured Clinical Interview Diagnostic (SCID) IV (Williams et al., 1992). Five MDD participants were taking antidepressants during scanning. These medications included: Zoloft, Prozac, Levothyroxine, Renlafaxin, Trazadone, Effexor and Wellbutrin. Three of the five participants that were on medications were on more than one medication. In addition, 14 of the 17 MDD participants were suffering a recurrent episode. Seven of the 17 MDD participants had a co-morbid diagnosis of anxiety, panic or social phobia, one participant had co-morbid diagnosis of an eating disorder, one participant had co-morbid diagnosis of PTSD and one participant had co-morbid diagnosis of schizophrenia. One MDD participant was excluded from the fMRI analysis because of poor segmented normalization (i.e., part of cortex was segmented off).

The Institutional Review Board of the University of Michigan approved this study and all participants provided informed consent as administered by the Institutional Review Board of the University of Michigan. Participants had to refrain from marijuana use for at least 6 months prior to participation and had to refrain from alcohol consumption at least 24 h prior to participation. Participants were also excluded if they had every used illicit drugs (i.e., cocaine, LSD). Participants were compensated $25/h for their participation.

fMRI acquisition and preprocessing parameters

Images were acquired on a GE Signa 3-Tesla scanner equipped with a standard quadrature head coil. Functional T2* weighted images were acquired using a spiral sequence with 40 contiguous slices with 3.44 × 3.44 × 3 mm voxels (repetition time (TR) = 2000 ms; echo time (TE) = 30 ms; flip angle = 90°; field of view (FOV) = 22 cm). A T1-weighted gradient echo anatomical overlay was acquired using the same FOV and slices (TR = 250 ms, TE = 5.7 ms, flip angle = 90°). Additionally, a 124-slice high-resolution T1-weighted anatomical image was collected using spoiled-gradient-recalled acquisition (SPGR) in steady-state imaging (TR = 9 ms, TE = 1.8 ms, flip angle = 15°, FOV = 25–26 cm, slice thickness = 1.2 mm).

Functional images were corrected for differences in slice timing using 4-point sinc-interpolation (Oppenheim et al., 1999) and were corrected for head movement using MCFLIRT (Jenkinson et al., 2002). To reduce noise from spike artifacts, the data were winsorized prior to normalization (Lazar et al., 2001) by exploring time courses for each voxel and finding values that were 3 standard deviations (SDs) away from the mean of that voxel's time course. Spikes that were above 3 SDs from the mean were made equal to the mean + 3 SDs and spikes that were 3 SDs below the mean were made equal to the mean − 3 SDs.

Each SPGR anatomical image was corrected for signal in-homogeneity and skull-stripped using FSL's Brain Extraction Tool (Smith et al., 2004). These images were then segmented with SPM5 (Wellcome Department of Cognitive Neurology, London) into gray matter, white matter and cerebrospinal fluid and normalization parameters for warping into MNI space were recorded. These normalization parameters were applied to the functional images maintaining their original 3.44 × 3.44 × 3 mm resolution, and then the functional images were spatially smoothed with a Gaussian kernel of 8 mm.

To correct for physiological artifacts all of our functional data underwent PHYCAA correction, which removes some known sources of physiological noise from the data (Churchill et al., 2012). This model estimates physiological noise components that originate from consistent brain regions, and have strong temporal autocorrelations. PHYCAA controls for both global sources of noise present in brain tissue (e.g. gray and white matters), and noise that is concentrated in the ventricles and major blood vessels (Churchill et al., 2012). This provides a more conservative approach to removing global noise in the brain, unlike standard mean regression (Fox et al., 2009), which may have a partly neuronal basis (Schölvinck, et al., 2010) and can distort connectivity patterns (Saad et al., 2012) particularly when comparing groups (Gotts et al., 2013). Lastly, corrections based on physiological models have been previously shown to reduce global confounds while simultaneously preserving functional connectivity relationships (Chang and Glover, 2009).

Furthermore, 24 motion parameters were calculated, which included the linear, squared, derivative, and squared derivative of the six rigid-body movement parameters (Lund et al., 2005). A principal component analysis was performed on these 24 motion parameters and only the first principal component, which accounted for nearly 90% of the motion variance, was covaried out from each voxel's time course to remove any signal that could be attributed to motion. Lastly, functional images were parceled into 116 different ROIs based on the AAL template for analysis.

Task parameters

Participants initially performed two resting-state scans back-to-back that were 8 min in length. Participants were instructed to look at a fixation cross at the center of the screen and were told not to think about anything in particular (i.e., they could think about whatever they wanted to). After acquiring anatomical images of the brain, participants were then taken out of the scanner and were asked to generate four negative autobiographical memories. In order to facilitate the

generation of the memories, we provided four distinct prompts such as "Please recall a specific time when you were rejected by someone you loved or still love" or "Please recall a specific time when you were very embarrassed." Following such a prompt, participants had to indicate whether they were able to think of a prompted event and if they were successful in doing so they were asked to re-live the event for 30 s as wells they could. Next, they had to rate how positively and negatively they felt about that event using a visual-analog scale (VAS). The raw VAS data was collected on a line of the length of 500 pixels. For the analysis these data were then converted into percentage values (0–100) for easier interpretation.[1] Finally, they were asked to describe the event in a few sentences and to create a 2 to 3 word long cue that reminded them of the event.

Following the creation of the events, participants went back into scanner. Only considering the two most negatively rated events, we simultaneously showed the event description and its cue and instructed participants to pair the two so that they were able to easily recall the memory after seeing the corresponding cue. In a next step, participants were asked to practice recalling the events after seeing the corresponding cue. For that purpose, participants had to press a key as soon as they were able to bring to mind the cued event. The cues were repeated until participants were able to vividly recall the corresponding event in less than 5 s.

Following this practice session, the induction period started. Participants were presented with a cue of one of the two memories that they rated as being most negative. The cue stayed on the screen for 3 min and participants were instructed to re-live that experience as vividly as possible in their imagination and to go back to the time and place of the experience in their imagination and to re-experience it happening to them all over again. After 3 min the cue of the second negatively rated event was presented on the screen. After this negative mood induction, participants again performed another resting-state scan where they fixated centrally on a fixation cross for 8 min and were instructed not to think about any particular memory. A schematic diagram of this procedure is shown in Fig. 1.

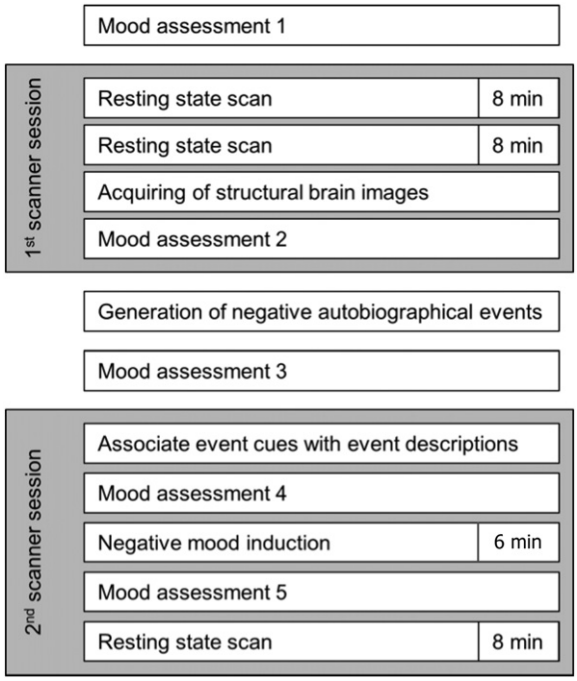

Fig. 1. Schematic task diagram: This figure shows the order of conditions and when the mood measurements were taken. Mood measurement 3 was not used in our analysis.

fMRI analysis parameters

Whole-brain fMRI timeseries were parcellated into 116 brain areas based on the automated anatomical labeling (AAL) template (Tzourio-Mazoyer et al., 2002). These timeseries were then correlated together to form a full correlation matrix for all regions correlated with all other regions for each subject and condition.

Partial Least Squares (PLS) analysis was then performed on these correlation matrices. PLS is a multivariate statistical method that is used to relate two sets of variables together. In the case of neuroimaging one set of variables could be brain data (e.g., BOLD signal per voxel per time point) while the other set of variables could be the experimental study design (e.g., groups and experimental conditions). The first step in PLS is to compute the covariance between the two sets of variables (i.e., the "cross-block" covariance). The second step of PLS is to perform a singular value decomposition on the "cross-block" covariance matrix to determine the combination of variables in each set that are optimally related to each other (i.e., that account for the greatest proportion of "cross-block" covariance). This combination, termed a latent variable (LV), is comprised of a linear combination (i.e., weighted) of variables from both sets (i.e., the brain and the experimental sets), as well as a scalar singular value. For the brain set this combination is a spatial–temporal pattern (saliences) and for the design set this is a contrast between groups and conditions. The mutually orthogonal LVs are extracted in order of magnitude, i.e., the first LV explains the most "cross-block" covariance and the second LV explains the second most "cross-block" covariance. In the present study the brain data were not activations (i.e., voxels in time), but were rather functional connections between the 116 AAL parcels. This produced 6670 unique connections (i.e., $(116 * 115) / 2$). As a result, the latent variable represents a weighted combination of functional connections that optimally relate to our groups and conditions (i.e., depressed vs. control for the 4 different experimental conditions).

The significance of each LV is assessed with permutation testing. A set of 500 permuted samples were created by randomly re-ordering subjects and condition labels without replacement for the brain set (note: groups and conditions are permuted because PLS is uncovering the weighted pattern of groups and conditions that explains the most covariance in the between the experimental conditions and brain connectivity) while the labels for the design set are maintained resulting in 500 new covariance matrices. These covariance matrices embody the null hypothesis and are then each subjected to singular value decomposition as before resulting in a null distribution of singular values. The significance of the original LV is assessed with respect to this null distribution and the p-value is calculated as the proportion of permuted singular values that exceed the original singular value. Critically, the permutation test involves the whole multivariate pattern, and only a single test is performed. As a result, correction for multiple comparisons is not needed (McIntosh and Lobaugh, 2004).

The reliability with which each functional connection expresses the LV pattern is determined with bootstrapping. A set of 500 bootstrap samples are created by re-sampling subjects with replacement within each condition (i.e., preserving condition labels, but not subject labels). Each new covariance matrix is subjected to singular value decomposition as before, and the saliences of the bootstrapped dataset are used to build a sampling distribution of the saliences from the original dataset. The purpose of a constructed bootstrapped sampling distribution is to determine the reliability of each salience; saliences that are highly dependent on which participants are included in the analysis will have wide distributions. A single index of reliability ("bootstrap" ratio) is calculated by taking the ratio of the salience to its bootstrap estimated standard error. A bootstrap ratio for a given functional connection is large when that functional connection has a large and stable salience. Importantly, bootstrap ratios are measures of reliability and robustness, but they are not used for statistical inference and do not

[1] Note: All mood measures were collected with the same VAS scale for both positive and negative affect.

involve any hypothesis testing. Thus, correction for multiple comparisons is not necessary. Moreover, bootstrap ratios provide a natural way of thresholding the final network maps, which show only those connections that exceed the 95% confidence interval of the bootstrap distribution.

To summarize, the design saliences are weights (analogous to loadings in principal component analysis) that index the contribution of different groups and/or conditions to a latent variable. Thus, the design saliences may be interpreted as the dominant, data-driven contrast in the data. For instance, in Fig. 5A, the design saliences are essentially 1 1 1 1 −1 −1 −1 −1, indicating primarily a group difference in functional connectivity. To interpret the contrast, and which group has greater connectivity, one must reference the corresponding bootstrap ratios. In Fig. 5B, all bootstrap ratios were positive, indicating that those functional connections express the contrast in Fig. 5A in a positive manner, i.e. greater functional connectivity for healthy controls relative to patients with MDD. Had there been any connections with negative bootstrap ratios, they would be interpreted as expressing the opposite contrast, i.e. greater functional connectivity for patients with MDD relative to healthy controls.

Behavioral PLS is a variant of PLS to examine the relationship between brain and behavior as a function of group and condition. In behavioral PLS the "cross-block" covariance is between the design variables and the correlation between brain and behavior. The LVs then reflect how group and conditions modulate brain and behavior relationships.

All of our analyses were performed on unthresholded correlation matrices because we wanted to preserve as much information from the correlation matrices as possible. In this way, it is definitely possible that a functional connection with a low magnitude would still be associated with a latent variable. Importantly however, the only way that this could happen is if that functional connection changed in a robust and reliable way, due to the experimental manipulations. Thus, a weak functional connection could still contribute to a latent variable if it was reliably stronger or weaker for one group versus another, or for one condition versus another.

Thus, our choice to use the original correlation matrices was primarily driven by the assumption that all statistically reliable changes in functional connectivity are meaningful, regardless of whether they involve or do not involve connections greater than some arbitrary threshold. Had we thresholded the correlation matrices, we would be assuming that group and condition effects are only expressed by high-magnitude, supra-threshold connections, eschewing the possibility of detecting any connections which go from being sub-threshold to supra-threshold, or vice versa.

Lastly, correlation distributions tend to be biased and therefore require a Fisher r-to-z transformation. However, this is only necessary for parametric tests and since PLS runs on resampling statistics, distributional assumptions are not necessary. As such performing a Fisher r-to-z transformation would yield identical results and therefore we chose not to perform the transformation on our correlation values.

Results

Behavioral results

A 2 (MDD vs. HC) × 4 [conditions: resting 1, resting 2, induced rumination and resting 3] ANOVA examined changes in positive and negative affect during the experiment. As expected, over the entire experiment, MDDs showed greater negative affect, $F(1,33) = 19.44$, $p < .001$, partial-eta$^2 = .37$, and less positive affect, $F(1,33) = 11.98$, $p < .005$, partial-eta$^2 = .27$ than non-depressed controls. Interestingly, we found a significant group * condition interaction for negative affect, $F(3,99) = 6.37$, $p < .001$, partial-eta$^2 = .16$, and a non-significant effect for positive affect, $F(3,99) = 2.06$, $p = .11$, partial-eta$^2 = .06$.

As shown in Fig. 2, this interaction was driven by changes in mood following the generation of negative events and the negative rumination induction, where mood in non-depressed controls became similar to individuals diagnosed with MDD.

When comparing the largest changes in mood (i.e., the difference in mood between resting 1 and resting 3), mood was significantly lowered (i.e., decreasing positive affect and increasing negative affect) for both groups: for the MDD group, the drop in positive affect $F(1,17) = 20.17$, $p < .001$, partial-eta$^2 = .54$ and the increase in negative affect $F(1,17) = 14.20$, $p < .005$, partial-eta$^2 = .46$ were both significant; and for the HC group the drop in positive affect $F(1,17) = 32.67$, $p < .001$, partial-eta$^2 = .67$ and the increase in negative affect $F(1,17) = 64.29$, $p < .001$, partial-eta$^2 = .80$ were both highly significant. HCs exhibited significantly larger changes in mood compared to MDDs following the negative mood induction, $F(1,33) = 3.65$, $p = .06$, partial-eta$^2 = .10$ for changes in positive mood and $F(1,33) = 11.93$, $p < .005$, partial-eta$^2 = .27$ for changes in negative mood. These behavioral results show that mood changes are not the same during unconstrained resting-state intervals as compared to induced ruminative state, which provides initial behavioral evidence that the two intervals (unconstrained rest vs. induced rumination) are not identical. More specifically, the ruminations that occur during unconstrained resting-intervals do not have the same impact on mood as explicitly induced ruminative states.

fMRI connectivity results from the seed analysis

To determine whether functional connectivity during unconstrained resting-state intervals was similar to active rumination, we conducted a first analysis that focused on the "default-mode" network. We used seeds from the left and right posterior cingulate cortex (PCC), a known member of the default-mode network (Fox and Raichle, 2007; Fox et al., 2005) and parcellated the brain into 116 areas with the Automated Anatomical Labeling (AAL) template (Tzourio-Mazoyer et al., 2002). For both the left and right PCC seeds we examined connectivity between each seed and the other 115 nodes in the network. We performed a multivariate analysis for changes in functional connectivity by group (MDD vs. HC) and condition (resting 1, resting 2, induced rumination and resting 3) using partial least squares (PLS) (Krishnan et al., 2011; McIntosh and Lobaugh, 2004; McIntosh and Misic, 2013), which determines the contrast of groups and conditions that explains the most covariance between functional connectivity and groups and conditions.

The results from this seeded PLS analysis are shown in Fig. 3. Fig. 3A displays the strongest effect in the data (i.e., latent variable), where the weightings on the groups and conditions explain the most covariance in functional connectivity. A high or low bar signifies a strong relationship between functional connectivity and that task condition and group. The first latent variable was highly significant for both the right-PCC seed, $p < .001$, and the left-PCC seed, $p < .005$, and explained over 57% of the covariance in the data (over 65% for the right-PCC seed and over 57% for the left-PCC seed).

This analysis revealed three salient effects. First, the participants diagnosed with depression are much more sensitive (in terms of functional connectivity) to the different conditions in the experiment, whereas the non-depressed participants are not as affected by the different conditions (i.e., highly overlapping error bars). This is interesting given that both groups showed large changes in mood for the different conditions.

Second, the induced rumination phase is different from the first resting-state interval for the participants' diagnosed with depression where the participant's with depression show reliable heightened connectivity when analyzed using the left-PCC seed ($p = 0.014$) and the right-PCC seed ($p = 0.02$[2]). These results suggest that the neural

[2] These tests were conducted as a separate PLS analysis containing only the resting 1 and induced rumination conditions and only the MDD group.

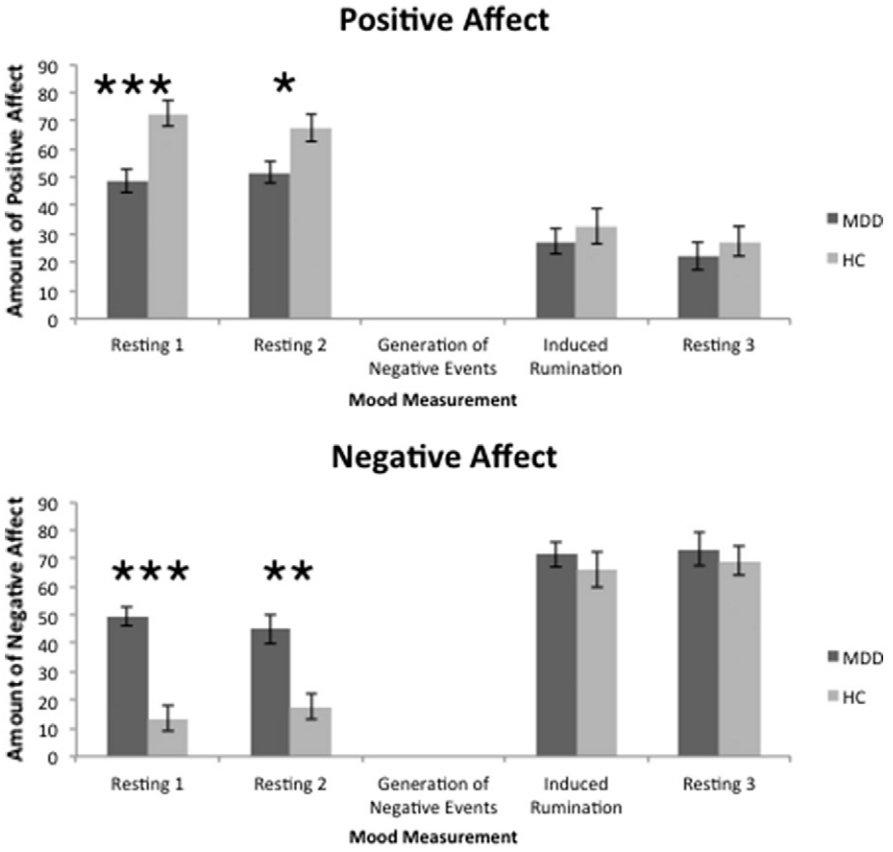

Fig. 2. Behavioral mood effects: How positive affect (top) and negative affect (bottom) change with the different experimental conditions for MDDs and HCs. The first mood measurement was taken before the first resting-state scan, the second mood measurement was taken after the second resting-state scan, the third mood measurement was taken after participants generated their negative autobiographical memories (but was not analyzed because this measurement was confounded by relief from being out of the scanner), the fourth mood measurement was taken after participants learned to associate cue words with their negative memories, and the fifth mood measurement was taken after participants actively recalled the negative memories. *** indicates a significant difference $p < .001$; ** indicates a significant difference $p < .01$; *indicates a significant difference $p < .05$.

processes of depressive rumination are not identical to the unconstrained resting-state intervals. Third, the results were nearly identical whether the left or right PCC was used as the seed.

Lastly, the first resting-state interval when participants first enter the fMRI scanner does not show the same connectivity as the next resting-state scan for participants diagnosed with depression. We tested the significance of this effect by performing a seeded-PLS analysis (with the left PCC seed) for the MDD group and included only the first two resting-state scans; the effect was highly significant, $p < .0001$. When the same analysis was performed for the healthy group there was no statistical difference in connectivity for the first two scans, $p > .17$. The same results are also found when using the right-PCC seed: significant differences for resting 1 vs. resting 2 for MDD group $p < .05$, and no significant differences for the control group $p > .27$. In addition, when we included both groups in the seeded PLS analysis and examined only the first two resting-state scans we found a significant LV. Namely, there were greater differences in the first two resting-state scans for MDDs compared to controls ($p = .008$, cross-block covariance = 91%). The same results are found with the right-PCC seed ($p = .004$, cross-block covariance = 87%).

However, when testing this interaction effect more directly, we subtracted the connectivity for resting 1 vs. resting 2 for each group and ran PLS on the difference matrices. When doing so we did not find a significant interaction. It seems that for the MDD group, first entering the fMRI environment has an effect, which suggests that in patients with depression, patterns of resting-state connectivity may change considerably during a scanning session. This effect may also be driven by past cognitive states before participants entered the scanner, as past cognitive states have been found to impact functional connectivity at "rest" (Waites et al., 2005). Importantly, these results must be interpreted with some caution, as the interaction effect was not significant, largely because the direction of the effect was similar for the healthy group, but with larger variance (see Fig. 3).

With PLS, we can also uncover the connections that exhibit this effect most reliably. Fig. 3B shows the connections that reliably express the effect demonstrated in Fig. 3A. Participants with depression show increased connectivity between the PCC and the: subgenual-cingulate cortex (SCC)/orbital frontal cortex (oFC), left and right inferior frontal gyri (iFG), left and right temporal cortices, left and right occipital cortices and left and right cerebella during induced rumination relative to the other conditions. All of the robust connections are shown in Table 1. While these results are reminiscent of some previous results of heightened connectivity between the PCC and SCC in depression (Berman et al., 2011; Greicius et al., 2007), they also show that the effects may be stronger when participants are forced to ruminate on a negative autobiographical memory, rather than engaging in unconstrained thinking during "rest."

Relationship between seeded functional connectivity and behavior

In addition to examining differences in seeded connectivity by group and condition, we also examined the relationship between changes in functional connectivity and changes in mood. To determine this relationship, we ran a behavioral PLS analysis in which mood scores that were collected close in time to the different experimental conditions were included in the analysis to find relationships between seeded functional connectivity, mood, condition, and group.

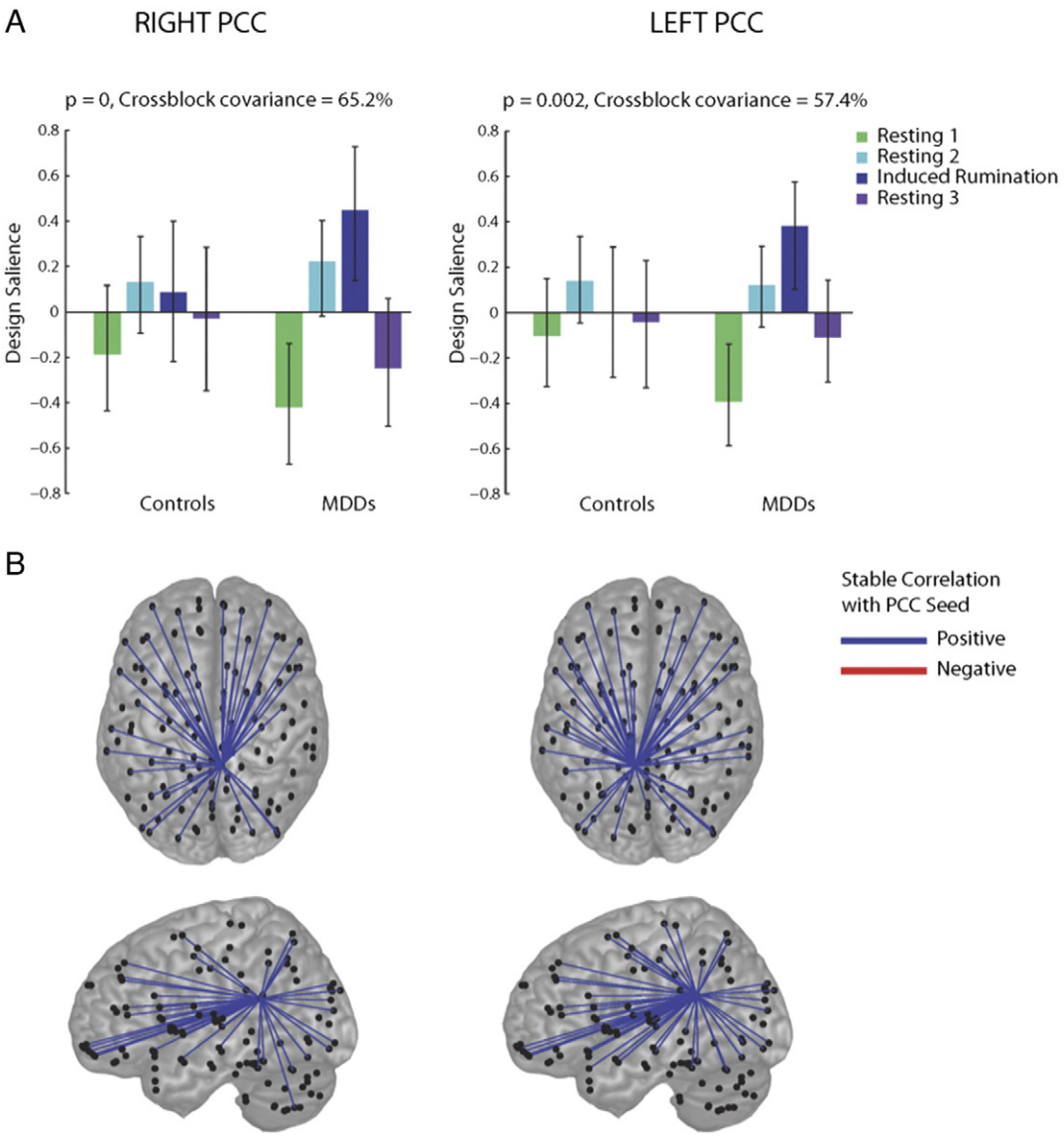

Fig. 3. Seed PLS results of the PCC: The latent variables (LV) from PLS are displayed for the right PCC seed and the left PCC seed. A high or low bar signifies a strong relationship between functional connectivity and that task condition and group. The results for both seeds are similar and show that connectivity is higher during the induced rumination phase for the MDDs (A). In addition, the experimental conditions seem to affect the MDDs more than the HCs. In the bottom panel (B) the functional connections that most reliably show the LV patterns, as determined by bootstrapping, are displayed for both the right- and left-PCC seeds. The connections in blue exhibit the direct LV pattern of increased connectivity during induced rumination for the MDDs.

Fig. 4 displays the results from that analysis. Fig. 4A shows the combination of group and conditions that maximizes the covariance between those conditions and seeded functional connectivity (a highly significant LV; $p = 0.004$, 63% cross-block covariance). The most reliable correlations between mood and functional connectivity were observed in the control group during induced rumination. In Fig. 4B we plot the connections that are most highly correlated with better mood (i.e., lower negative affect from the VAS) during induced rumination and also during the resting-state scan after induced rumination. While both groups show similar patterns during induced rumination, the patterns are quite different in the resting-state scan after induced rumination (see Fig. 4B resting 3). These effects are exacerbated in the global functional connectivity analyses presented in the next sections.

fMRI connectivity results from global analysis

Results from the seeded PLS analysis demonstrated that unconstrained thinking during rest does not exhibit the same functional connectivity patterns as active rumination for MDDs, but does not present reliable differences for HCs. Areas that have been known to be hyper-connected or hyper-active for individuals with MDD, such as SCC (Berman et al., 2011; Drevets et al., 2008; Greicius et al., 2007; Mayberg et al., 2005; Sheline et al., 2009a), were also found to show greater functional connectivity during periods of active rumination.

Seeded analyses, while highly informative, characterize the connectivity of a single brain area and do not capture how other, non-seed areas, are connected with each other. In this way, seeded analyses may be restrictive by focusing on connectivity in one network rather than on how all brain networks may be affected by different groups or experimental manipulations.

To address this issue, we performed a second analysis to examine how the complete connectivity profile differed between MDDs and HCs for the four different conditions in our experiment. We compared the full connectivity matrix between the two groups, again utilizing PLS. Fig. 5 shows the group-averaged correlation matrices as a reference. In the conducted PLS analysis individual participant matrices were used, not the group-averaged matrices. The results from the PLS analysis of global functional connectivity are shown in Fig. 6.

Table 1
Reliable connections from seed analysis. Listed in the table are the connections between AAL brain parcels that reliably change (i.e., bootstrap ratios greater than 2.5) according to the first LV of the seeded analysis. The first column shows the reliable connections with the left-PCC seed and the second column shows the reliable connections with the right-PCC seed. The L and R suffixes explain which hemisphere the parcel is in.

Left PCC seed	Right PCC seed
Precentral_L	Precentral_L
Precentral_R	Precentral_R
Frontal_Sup_R	Frontal_Sup_R
Frontal_Sup_Orb_L	Frontal_Sup_Orb_L
Frontal_Sup_Orb_R	Frontal_Sup_Orb_R
Frontal_Mid_L	Frontal_Mid_L
Frontal_Mid_R	Frontal_Mid_R
Frontal_Mid_Orb_L	Frontal_Mid_Orb_L
Frontal_Mid_Orb_R	Frontal_Mid_Orb_R
Frontal_Inf_Oper_L	Frontal_Inf_Oper_L
Frontal_Inf_Oper_R	Frontal_Inf_Oper_R
Frontal_Inf_Tri_L	Frontal_Inf_Tri_L
Frontal_Inf_Tri_R	Frontal_Inf_Tri_R
Rolandic_Oper_L	Supp_Motor_Area_R
Supp_Motor_Area_L	Olfactory_R
_Motor_Area_R	Frontal_Mid_Orb_R
Olfactory_L	Insula_R
Olfactory_R	Hippocampus_R
Insula_L	Amygdala_R
Insula_R	Occipital_Sup_L
Hippocampus_L	Occipital_Sup_R
Hippocampus_R	Occipital_Mid_L
Amygdala_L	Occipital_Mid_R
Amygdala_R	Occipital_Inf_L
Lingual_L	Occipital_Inf_R
Occipital_Sup_L	Fusiform_L
Occipital_Sup_R	Parietal_Sup_L
Occipital_Mid_L	Parietal_Sup_R
Occipital_Mid_R	Parietal_Inf_L
Occipital_Inf_L	SupraMarginal_L
Occipital_Inf_R	Precuneus_L
Fusiform_L	Caudate_L
Postcentral_L	Caudate_R
Postcentral_R	Putamen_L
Parietal_Sup_L	Putamen_R
Parietal_Sup_R	Pallidum_L
Parietal_Inf_L	Pallidum_R
SupraMarginal_L	Thalamus_L
SupraMarginal_R	Thalamus_R
Paracentral_Lobule_L	Temporal_Sup_L
Paracentral_Lobule_R	Cerebellum_4_5_L
Caudate_L	Cerebellum_6_L
Caudate_R	Cerebellum_7b_L
Putamen_L	Vermis_6
Putamen_R	
Pallidum_L	
Pallidum_R	
Thalamus_L	
Thalamus_R	
Heschl_L	
Temporal_Sup_L	
Temporal_Sup_R	
Temporal_Pole_Sup_L	
Temporal_Mid_R	
Cerebellum_4_5_L	
Cerebellum_6_L	
Cerebellum_6_R	
Vermis_6	

As shown in Fig. 6A, there is a very strong effect of group in which the healthy group exhibits overall greater functional connectivity compared to the MDD group, independent of condition ($p = 0.014$, 93% cross-block covariance). This increase in functional connectivity for HCs was observed throughout the whole brain as shown in Fig. 6B where connections in blue show reliably increased connectivity for HCs and connections in red show increased connectivity for MDDs (note: there were no such connections). As can be seen, there are many connections that show overall greater connectivity for the HCs. Importantly, this powerful group effect had been completely masked in the seeded analysis.

There may be some concerns that differences in timing for the different conditions could be affecting our results because the first two resting-state scans are longer (8 min) than the induced rumination condition (6 min). In addition, the rumination condition has participants thinking about 2 different memories (1 memory for the first 3 min and another memory for the second 3 min). To abate these concerns we analyzed the first 3 min of each condition and find the same pattern of results of hypo-connectivity for the MDD group relative to the HC group across all of the conditions ($p = .03$, cross-block covariance = 87%).

To determine whether there was any effect of condition in the global connectivity analysis, we removed all potential group effects (that dominated the differences between the groups) by subtracting the group means for each group separately prior to the PLS analysis. When doing so we found a non-significant effect ($p = 0.07$ cross-block covariance = 37.59%), but the pattern mirrored that of the seed analysis results of heightened connectivity for MDDs during induced rumination. This means that while the effect of condition on functional connectivity was stronger for brain networks that were connected to the PCC (such as the default mode network), the impact of condition on MDDs is also seen when the full brain connectivity profile is examined. In summary, for both analyses, functional connectivity is more likely to change by condition for patients with depression compared to controls; but both of these effects are smaller than the main effect of group on global connectivity.

Relationship between global functional connectivity and behavior

Finally, we investigated the relationship between overall functional connectivity and changes in mood. To determine this relationship, we ran a behavioral PLS analysis, but this time used the full connectivity profile to find relationships between global functional connectivity, mood, condition, and group. Fig. 7 displays the averaged correlation matrices between mood and connectivity for both groups. It is apparent from those matrices that the relationship between mood and connectivity differs for the two groups (particularly in resting 3).

The first significant effect from the behavioral PLS analysis is shown in Fig. 8A ($p = 0.006$, 54% cross-block covariance). Interestingly, the strongest correlations between mood and functional connectivity were observed during the induced rumination phase and, to a lesser extent, during the third resting-state scan, but fewer reliable relationships between mood and functional connectivity were observed during the first two resting-state scans. This effect is very salient when examining the correlation between strength of functional connectivity and negative mood scores, which are shown in Fig. 7, where the most positive correlations are in the induced rumination condition for both groups.

Fig. 8B shows the functional connections that were reliably correlated with negative mood and how these brain–behavior relationships differ between the two groups. During induced rumination, the HC group exhibited strong relationships between mood and connectivity for anterior–posterior connections in a more "ventral" network, while the MDD group exhibited strong relationships for anterior–posterior connections in a more "dorsal" network. For both groups increased connectivity in those areas was related to lower negative mood as assessed with the negative affect VAS score (i.e., better mood).

When examining the resting-state interval directly following the induced rumination phase, we observed even stronger differences between the groups. This resting-state interval is not as unconstrained as the first two resting scans as it is highly contaminated by the negative mood induction. However, it offers an opportunity to examine how both groups may regulate mood neurally after the rumination induction. The HC group exhibited strong correlations between functional connectivity and mood for anterior–posterior connections, and in particular high connectivity in the occipital cortex. High connectivity in those areas

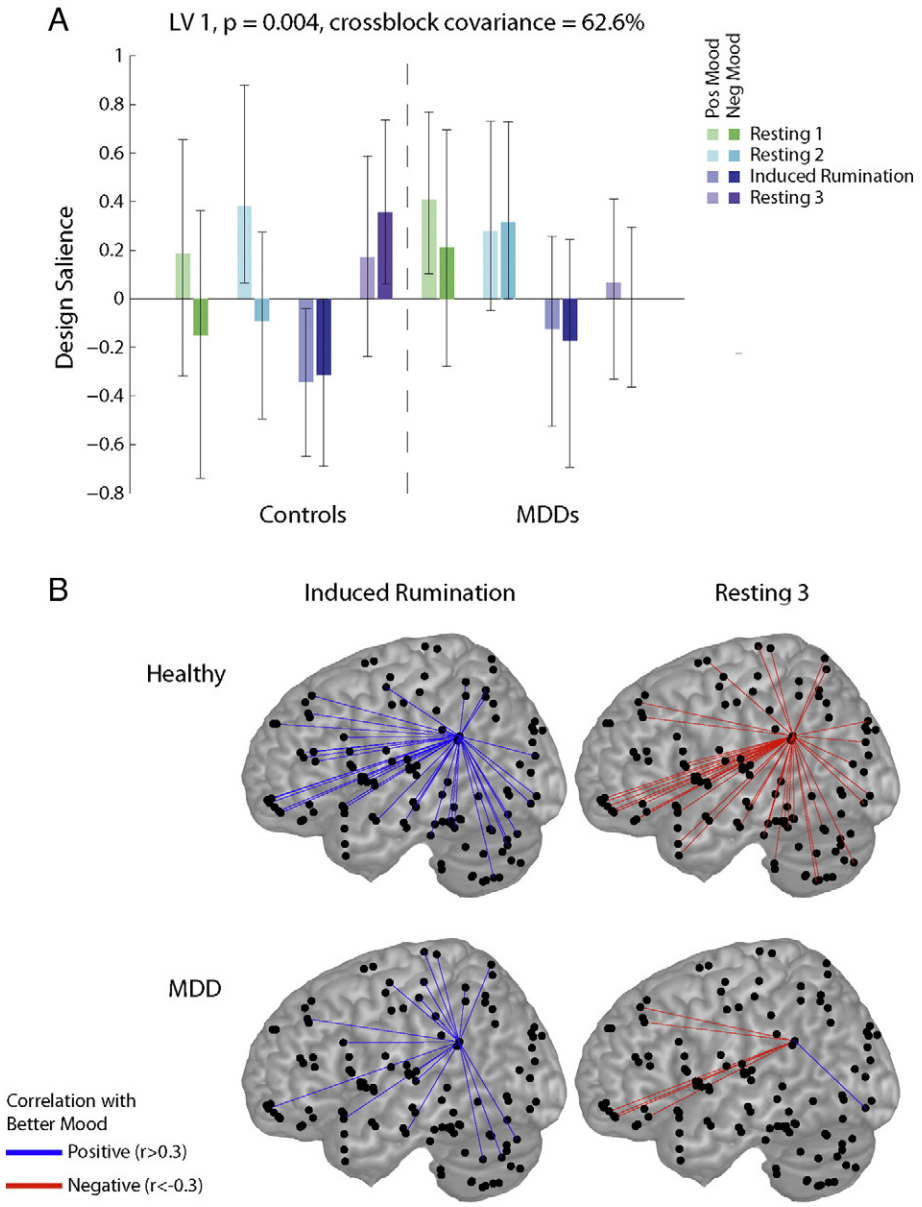

Fig. 4. PLS analysis relating seeded connectivity and mood: (A) shows the group and condition differences in the relationship between seeded connectivity and mood. Mood was only reliably related to connectivity during the induced rumination phase for both positive and negative mood. (B) shows the connections that are most reliably related to better mood (i.e., decreased negative affect) for the induced rumination phase and the resting-state scan after induced rumination (mood measures 4 and 5), as determined by bootstrap analysis.

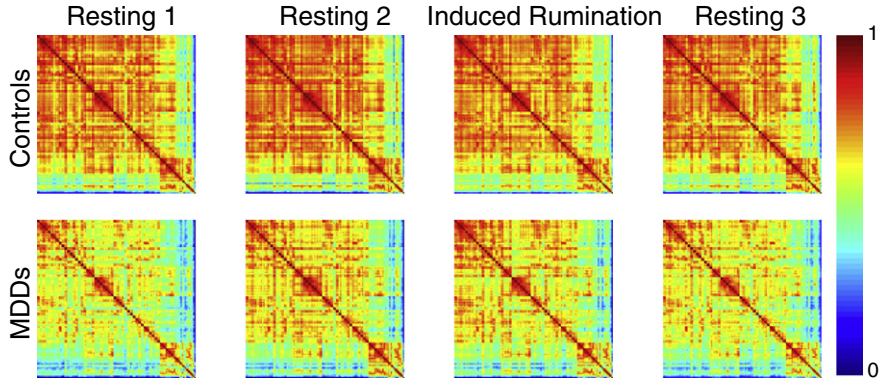

Fig. 5. Group averaged correlation matrices by group and condition: For illustrative purposes we display the group averaged correlation matrices for each group and condition. The range is from 0 to 1.

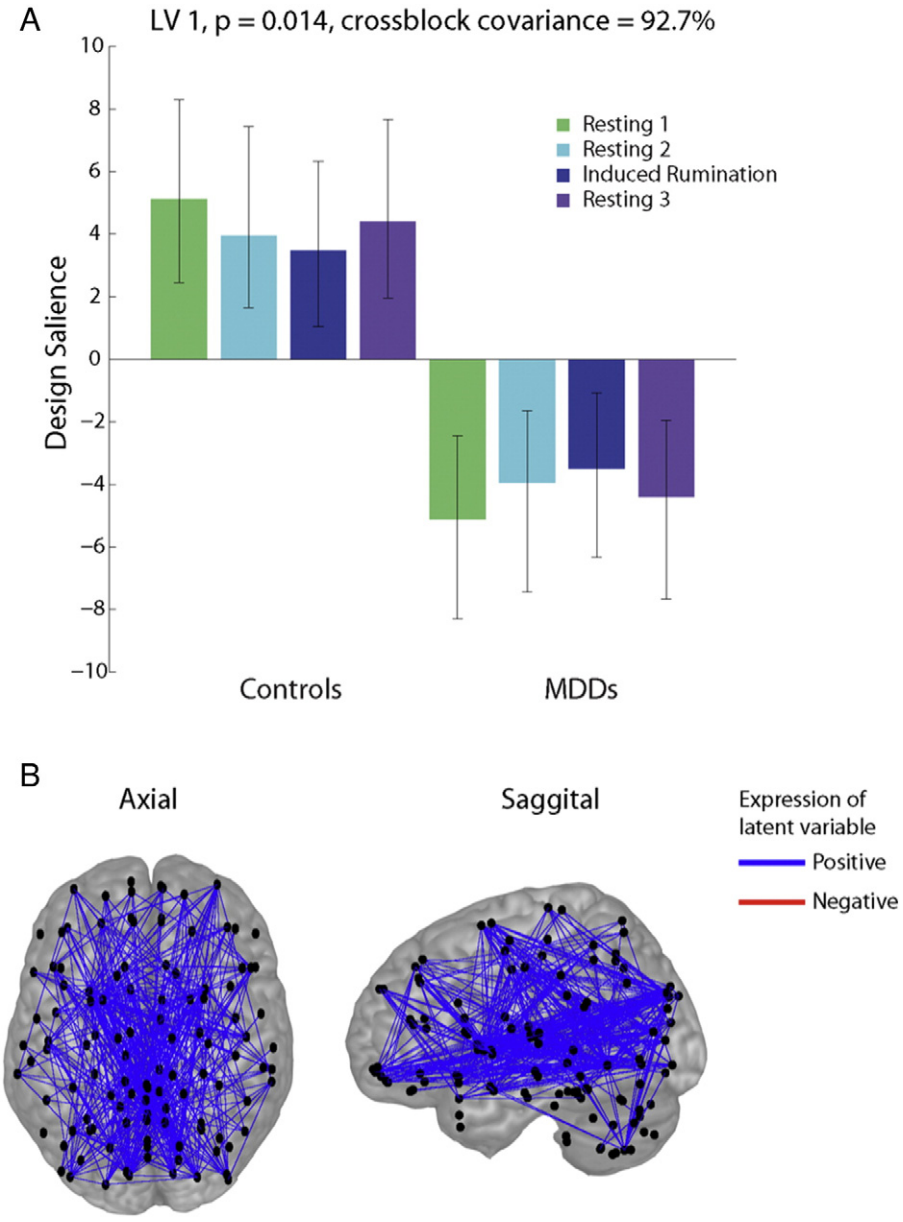

Fig. 6. PLS results from global connectivity: PLS LV showing the dominant differences in connectivity. (A) Dominant differentiation of groups and conditions. (B) Functional connections that reliably express the group difference shown in (A).

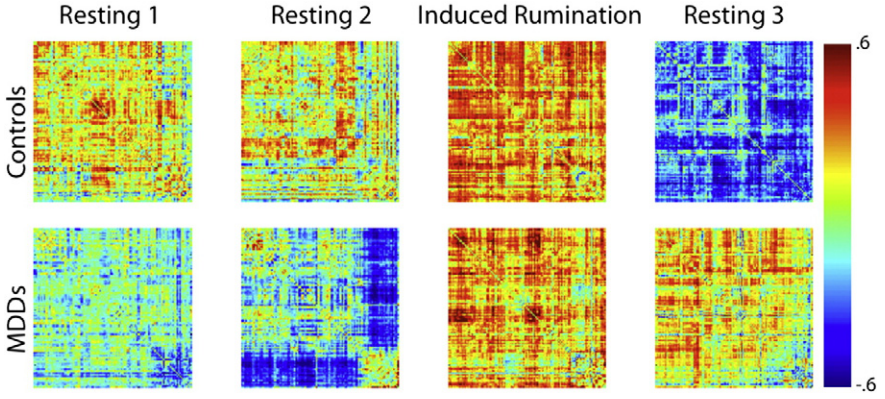

Fig. 7. Relationship between mood and connectivity: Group averaged correlation matrices showing the correlation between negative affect and functional connectivity for both groups and each condition. One can see the strong correlation between mood and connectivity in the induced rumination condition, with a subsequent reversal in correlation during resting 3 for the controls. The range of correlation is between −.6 and +.6.

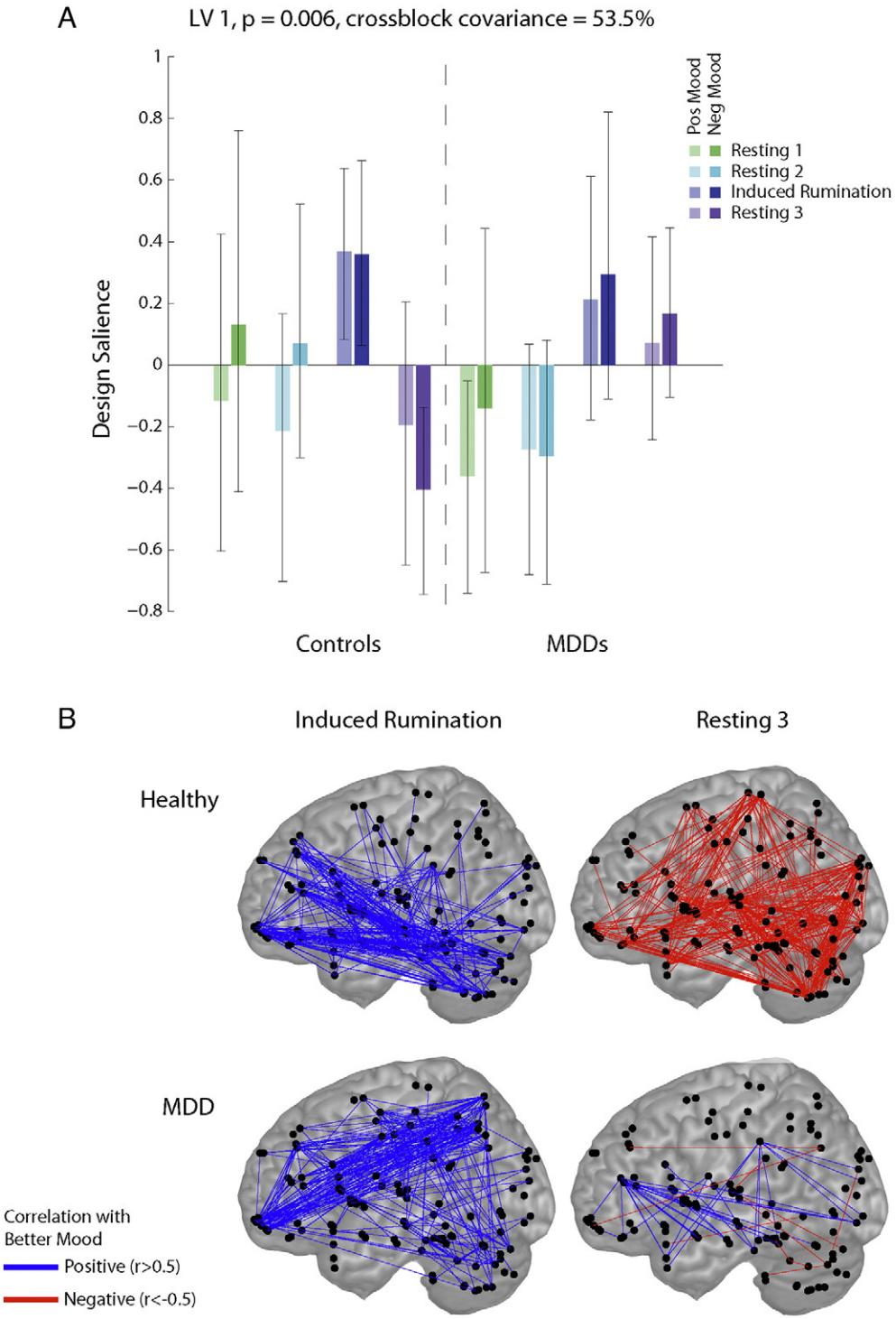

Fig. 8. PLS analysis relating global connectivity and mood: (A) shows the group and condition differences in the relationship between connectivity and mood. Mood was only reliably related to connectivity during the induced rumination phase for both positive and negative mood (determined by bootstrap analysis). (B) Shows the connections that are most reliably related to negative mood for the induced rumination phase and the resting-state scan after induced rumination (mood measures 4 and 5).

was related to increased negative mood. This is interesting because it is possible that high connectivity with occipital–temporal areas may be a neural mechanism of high visualization of the negative memory, so showing weaker connectivity in those areas may be related to improved mood and serve as a beneficial mood-regulation strategy. For the MDD group there are few connections that significantly correlate with mood, which suggests that MDDs are more inconsistent in their relationships between connectivity and mood following induced rumination.

Results with a different parcellation scheme

All of the global results were found utilizing the AAL parcellation scheme. One may wonder if our results are idiosyncratic to this parcellation scheme or if these global results might generalize to another parcellation scheme. Smith et al. (2011) caution the use of atlas-based ROIs, which may not match functional ROI boundaries and could lead to poor results. As such, we analyzed our data using a second parcellation scheme that was based on meta-analyses of

fMRI studies (please see Dosenbach et al., 2010 for a more in-depth description) to build a functionally defined set of ROIs that would cover much of cerebral cortex and the cerebellum (Dosenbach et al., 2010).

Results from the meta-analysis of Dosenbach et al. (2010) yielded 160 peaks and we drew 10 mm diameter spheres around each of those peaks to define our new ROIs for this functionally defined parcellation scheme. Fig. S1 displays the (Dosenbach et al., 2010) ROIs overlaid on top of the AAL atlas ROIs. We extracted the mean timeseries from each of these ROIs and re-ran the two global analyses. Importantly, we obtained nearly the identical results utilizing this functionally defined parcellation scheme where we find heighted connectivity for the control group compared to the MDD group, $p = 0.016$, cross-block covariance = 84.7%. These results are also plotted in Fig. S2.

In addition, we also found a similar LV pattern when examining the relationship between the mood measures and global connectivity utilizing the functionally defined ROIs, where mood and connectivity were reliably related, $p = 0.004$, cross-block covariance = 38.7%. The greatest correspondence between connectivity and behavior was found during the induced rumination condition and the resting 3 condition for the healthy group. The fact that both of these results were nearly identical for another parcellation scheme suggests that the results are robust and are not idiosyncratic to how the brain is divided.

Discussion

The first goal of this study was determine whether unconstrained resting-state intervals were similar to induced ruminative states behaviorally and neurally. We interrogated this question with a novel experimental paradigm and novel network analyses (i.e., PLS applied to global functional connectivity) to examine the similarity of brain networks during unconstrained resting-state intervals and induced ruminative states.

First, mood was significantly altered between unconstrained resting-state intervals and induced-ruminative states indicating, that behaviorally, these cognitive states are not synonymous. This effect may not be surprising for the HC group, but does show that unconstrained thought patterns for MDDs are not synonymous with active rumination and given that it is assumed that MDD's ruminate during rest, this effect is important. Second, with multivariate seeded analyses with the PCC we found heightened connectivity for the MDD group compared to the control group during induced ruminative states compared to resting states. These results again signal that induced ruminative states are not the same as unconstrained resting-state intervals, particularly for individuals with depression.

While both groups showed significant changes in mood from unconstrained states to ruminative states, HC brain networks remained relatively unchanged for these different conditions. On the other hand MDD brain networks did significantly change for the different conditions and showed exacerbated connectivity in default-network areas, including the Subgenual Cingulate Cortex (SCC) during induced rumination. The fact that HCs show changes in subjective mood, but maintain similar brain connectivity for unconstrained and ruminative states suggests that HCs may have neural networks that may aid more strongly in mood regulation compared to MDDs, which may prevent future rumination. These results are similar to previous research showing failures to down-regulate default-mode network activity when faced with negative stimuli and overall heightened default-mode network activation when faced with negative stimuli in depression (Sheline et al., 2009b). More generally, this heightened connectivity could reflect excessive self-directed thought (Buckner et al., 2008; Leech and Sharp, 2013; Raichle et al., 2001) in MDD.

Third, resting-state connectivity in the default-mode network on its own differed between the two groups, such that back-to-back resting state scans produced differences in connectivity for the MDD group, but not for the HC group, though some caution should be taken in the interpreting these results as the interaction was not found to be significant for group by resting 1 & 2. This result could mean that HCs are overall more stable in their functional connectivity compared to MDDs, and that MDDs may be more affected by the scanning environment compared to HCs. Therefore, one should not assume that MDDs will produce stable connectivity patterns during unconstrained states in the default-mode network.

Fourth, when examining global functional connectivity differences between the two groups we found significant differences between MDDs and HCs in overall connectivity. HCs exhibited overall higher connectivity across the whole brain and similar results have been found by other researchers studying depression with whole-brain networks (Veer et al., 2010). These results in combination with our seeded analysis results may help to reconcile results in the literature where some find increased connectivity (Berman et al., 2011; Broyd et al., 2009; Greicius et al., 2007; Sheline et al., 2010) in depression and others find decreases (Veer et al., 2010). These results imply that MDDs have increased connectivity in default-mode network areas, but decreased connectivity elsewhere. Such results have important implications when designing interventions to decrease rumination in depression. For example, interventions, either pharmacological or behavioral, that are tailored to increase overall connectivity while simultaneously decreasing connectivity in the default-mode network may be the most therapeutic. Certainly more research needs to be done to determine how altering connectivity in these networks would alter depressive symptoms, but this and other research are a starting point to identify dysfunctional networks in MDD.

Similar global drops in connectivity have also been found when comparing HCs and schizophrenic patients (Lynall et al., 2010) where schizophrenic patients showed an overall drop in connectivity compared to healthy controls. Other research in MDD has also suggested the importance of examining global functional connectivity as global functional connectivity has been found to be a highly sensitive metric in distinguishing depressed and healthy individuals (Zeng et al., 2012). As such, an overall drop in global functional connectivity may be emblematic psychopathology more generally. In our data, these results would have been missed if seed-based analyses had only been employed.

In related work, Harrison et al. (2008) examined changes in functional connectivity in a group of healthy individuals when thinking continuously about neutral vs. sad autobiographical memories. In this work, the authors found an increase in functional connectivity in a paralimbic network for sad vs. neutral recall and a decrease in functional connectivity in the default mode network for sad vs. neutral recall. The decreased connectivity in the default mode network was thought to reflect increased effort for healthy individuals when thinking about negative information. Our results align nicely with these results as we found heightened connectivity in the default mode network during induced rumination for the MDD group relative to the healthy group suggesting that overt rumination for them is less effortful compared to the healthy group. Of course, more work is needed to disentangle effort from rumination, but these results and those of Harrison et al. (2008) seem to point to similar conclusions.

Fifth, significant relationships between mood and functional connectivity were most strongly observed during induced rumination and the resting-state interval after the induced rumination phase. This was further evidence that unconstrained "resting-states" differ from active rumination states. This is not to say that rumination does not occur during "resting-states," but potentially the degree or foci of such rumination may differ when individuals are induced to ruminate. The relationship between mood and functional connectivity was also strongest when using global functional connectivity metrics rather than seeded connectivity metrics again demonstrating the utility of the global connectivity measure.

We observed striking group differences in how connectivity was related to mood during active rumination and also during the resting-state phase after induced rumination, which would be heavily influenced

from the negative rumination induction. Not surprisingly, carryover effects of previous mental states have been found to affect resting-state connectivity (Barnes et al., 2009). While both groups exhibited similar drops in mood during induced rumination, the networks that may support mood regulation appear to be quite different between the groups. HCs showed heightened connectivity in a more dorsal network, while MDDs showed heightened connectivity in a more ventral network. These findings are somewhat consistent with recent findings showing increased nodal centralities in medial frontal and parietal areas in MDD (Zhang et al., 2011), i.e., some of the same regions where we find heightened connectivity related to mood during induced rumination for MDD. In addition, Ma et al. (2013) have shown that connectivity between the cerebellum and the anterior cingulate, the ventromedial pre-frontal cortex, vetrolateral pre-frontal cortex and the temporal lobe strongly distinguishes MDD from non-MDD groups. Consistent with this finding are our results showing heightened connectivity between these areas that was related to mood for the healthy group. Counter-intuitively, HCs exhibited many connections that were correlated with mood post-induced rumination, while MDDs did not. However, the connections between connectivity and mood were different during and after rumination for the HCs and may provide a neural mechanism as to why HCs can recover from negative mood states, but MDDs have more difficulty.

We did have a heterogeneous MDD population in this study, which may have added noise to our results. However, even with this heterogeneous sample, we still found highly reliable and robust effects. In the future it would be interesting to see if there are differences in connectivity within the MDD group based on medication, co-morbid diagnosis and MDD recurrence. We our confident that our results are not driven by individual MDD participants because of the PLS resampling framework that tests for the robustness of the effects based on which participants are included/excluded from the analysis.

There could be other factors that may contribute to differences in connectivity between the groups. One such factor could be arousal levels. For example, lower connectivity between MDDs vs. non-depressed controls could be driven by lower arousal levels, but lower arousal levels characterize depression (i.e., these are not trivial factors to de-couple). Therefore, one would need an experiment that manipulated arousal levels, while not altering mood; a task that would not be easily accomplished. Importantly, if arousal was a main contributing factor, greater differences would be expected between groups during the final resting-state scan, but the largest condition differences were found during induced rumination, a condition that occurred earlier in the experiment. Lastly, the fact that global connectivity did not differ by condition suggests that arousal levels, task vigilance and fatigue were not factors contributing to our results.

Others may worry that lower global connectivity may reflect differences in motion or other physiological parameters. We are confident that motion is not a contributing factor because we covaried out motion from the functional timeseries and the 6-rigid body motion parameters were not significantly different between the two groups. We encourage readers to view recent work by Zeng et al. (2014) showing that motion may actually reflect neurobiological signal and therefore should not be regressed out with caution. In addition, our use of PHYCAA (Churchill et al., 2012) to remove physiological noise parameters from all participants should mitigate concerns that differences in connectivity were due to physiology. Our sample size was also relatively small because it was challenging to recruit our MDD sample, which is a limitation of the current study. However, the effects that we did obtain were robust under stringent bootstrapping and permutation tests, which should ease concerns regarding our sample size.

Our results show that when examining changes in functional connectivity in relation to health and disease, it is important to explore both specific neural networks such as those from our seeded analysis and the entire functional connectivity landscape, which revealed strong connectivity difference between groups. Therefore, we strongly encourage researchers to examine and report results from global connectivity in addition to results from singular networks.

Ironically, induced ruminative states led to stronger functional connectivity differences between the groups even though the subjective mood states between groups were more similar to one another during induced ruminative states. This result suggests that subjective feelings may manifest themselves quite differently neurally between the two groups. Lastly, while rumination may occur during unconstrained resting-state intervals the connectivity patterns are heightened during induced rumination in addition to the relationships with mood. Therefore, resting-state intervals do not identically reflect depressive rumination neurally or behaviorally.

Acknowledgments

This work was supported in part by a National Institute of Mental Health grant NIMH 60655 to John Jonides. We would like to thank Catherine Cherny for her help with data collection.

Appendix A. Supplementary data

Supplementary data to this article can be found online at http://dx.doi.org/10.1016/j.neuroimage.2014.09.027.

References

Barnes, A., Bullmore, E.T., Suckling, J., 2009. Endogenous human brain dynamics recover slowly following cognitive effort. Plos One 4 (8). http://dx.doi.org/10.1371/journal.pone.0006626.

Beck, A.T., Steer, R.A., Brown, G.K., 1996. Manual for the Beck Depression Inventory II (BDI-II). Psychological Corporation, San Antonio, TX.

Berman, M.G., Peltier, S., Nee, D.E., Kross, E., Deldin, P.J., Jonides, J., 2011. Depression, rumination and the default network. Soc. Cogn. Affect. Neurosci. 6 (5), 548–555. http://dx.doi.org/10.1093/scan/nsq080.

Bohr, I.J., Kenny, E., Blamire, A., O'Brien, J.T., Thomas, A.J., Richardson, J., Kaiser, M., 2012. Resting-state functional connectivity in late-life depression: higher global connectivity and more long distance connections. Front. Psychiatry 3, 116-116. http://dx.doi.org/10.3389/fpsyt.2012.00116.

Broyd, S.J., Demanuele, C., Debener, S., Helps, S.K., James, C.J., Sonuga-Barke, E.J.S., 2009. Default-mode brain dysfunction in mental disorders: a systematic review. Neurosci. Biobehav. Rev. 33 (3), 279–296. http://dx.doi.org/10.1016/j.neubiorev.2008.09.002.

Buckner, R.L., Andrews-Hanna, J.R., Schacter, D.L., 2008. The brain's default network: anatomy, function, and relevance to disease. Ann. N. Y. Acad. Sci. 1124, 1–38. http://dx.doi.org/10.1196/annals.1440.011.

Chang, Glover, 2009. Effects of model-based physiological noise correction on default mode network anti-correlations and correlations. NeuroImage 47 (4), 1448–1459.

Churchill, N.W., Yourganov, G., Spring, R., Rasmussen, P.M., Lee, W., Ween, J.E., Strother, S.C., 2012. PHYCAA: data-driven measurement and removal of physiological noise in BOLD fMRI. Neuroimage 59 (2), 1299–1314. http://dx.doi.org/10.1016/j.neuroimage.2011.08.021.

Dosenbach, N.U.F., Nardos, B., Cohen, A.L., Fair, D.A., Power, J.D., Church, J.A., Nelson, S.M., Wig, G.S., Vogel, A.C., Lessov-Schlaggar, C.N., Barnes, K.A., Dubis, J.W., Feczko, E., Coalson, R.S., Pruett, J.R., Barch, D.M., Petersen, S.E., Schlaggar, B.L., 2010. Prediction of individual brain maturity using fMRI. Science 329, 1358–1361.

Drevets, W.C., Price, J.L., Furey, M.L., 2008. Brain structural and functional abnormalities in mood disorders: implications for neurocircuitry models of depression. Brain Struct. Funct. 213 (1–2), 93–118. http://dx.doi.org/10.1007/s00429-008-0189-x.

Fox, M.D., Raichle, M.E., 2007. Spontaneous fluctuations in brain activity observed with functional magnetic resonance imaging. Nat. Rev. Neurosci. 8 (9), 700. http://dx.doi.org/10.1038/nrn2201 ER.

Fox, M.D., Snyder, A.Z., Vincent, J.L., Corbetta, M., Van Essen, D.C., Raichle, M.E., 2005. The human brain is intrinsically organized into dynamic, anticorrelated functional networks. Proc. Natl. Acad. Sci. U. S. A. 102 (27), 9673. http://dx.doi.org/10.1073/pnas.0504136102 ER.

Fox, et al., 2009. The global signal and observed anticorrelated resting state brain networks. J. Neurophysiol. 101 (6), 3270–3283.

Gotts, S.J., Saad, Z.S., Jo, H.J., Wallace, G.L., Cox, R.W., Martin, A., 2013. The perils of global signal regression for group comparisons: a case study of Autism Spectrum Disorders. Front. Hum. Neurosci. 7. http://dx.doi.org/10.3389/fnhum.2013.00356.

Greicius, M.D., Flores, B.H., Menon, V., Glover, G.H., Solvason, H.B., Kenna, H., Schatzberg, A.F., 2007. Resting-state functional connectivity in major depression: abnormally increased contributions from subgenual cingulate cortex and thalamus. Biol. Psychiatry 62 (5), 429. http://dx.doi.org/10.1016/j.biopsych.2006.09.020 ER.

Hamilton, J.P., Furman, D.J., Chang, C., Thomason, M.E., Dennis, E., Gotlib, I.H., 2011. Default-mode and task-positive network activity in major depressive disorder: implications for adaptive and maladaptive rumination. Biol. Psychiatry 70 (4), 327–333. http://dx.doi.org/10.1016/j.biopsych.2011.02.003.

Harrison, B.J., Pujol, J., Ortiz, H., Fornito, A., Pantelis, C., Yucel, M., 2008. Modulation of brain resting-state networks by sad mood induction. Plos One http://dx.doi.org/10.1371/journal.pone.0001794.
Jenkinson, M., Bannister, P., Brady, M., Smith, S., 2002. Improved optimization for the robust and accurate linear registration and motion correction of brain images. Neuroimage 17 (2), 825. http://dx.doi.org/10.1006/nimg.2002.1132.
Krishnan, A., Williams, L.J., McIntosh, A.R., Abdi, H., 2011. Partial Least Squares (PLS) methods for neuroimaging: a tutorial and review. Neuroimage 56 (2), 455–475. http://dx.doi.org/10.1016/j.neuroimage.2010.07.034.
Lazar, N.A., Eddy, W.F., Genovese, C.R., Welling, J., 2001. Statistical issues in fMRI for brain imaging. Int. Stat. Rev. 69 (1), 105.
Leech, R., Sharp, D.J., 2013. The role of the posterior cingulate cortex in cognition and disease. Brain http://dx.doi.org/10.1093/brain/awt162.
Lund, T.E., Norgaard, M.D., Rostrup, E., Rowe, J.B., Paulson, O.B., 2005. Motion or activity: their role in intra- and inter-subject variation in fMRI. Neuroimage 26 (3), 960. http://dx.doi.org/10.1016/j.neuroimage.2005.02.021.
Lynall, M.-E., Bassett, D.S., Kerwin, R., McKenna, P.J., Kitzbichler, M., Muller, U., Bullmore, E., 2010. Functional connectivity and brain networks in schizophrenia. J. Neurosci. 30 (28), 9477–9487. http://dx.doi.org/10.1523/jneurosci.0333-10.2010.
Ma, Q.M., Zeng, L.L., Shen, H., Liu, L., Hu, D.W., 2013. Altered cerebellar–cerebral resting-state connectivity reliably identifies major depressive disorder. Brain Res. 1495.
Mayberg, H.S., Lozano, A.M., Voon, V., McNeely, H.E., Seminowicz, D., Hamani, C., Kennedy, S.H., 2005. Deep brain stimulation for treatment-resistant depression. Neuron 45 (5), 651. http://dx.doi.org/10.1016/j.neuron.2005.02.014.
McIntosh, A.R., Lobaugh, N.J., 2004. Partial least squares analysis of neuroimaging data: applications and advances. Neuroimage 23, S250–S263. http://dx.doi.org/10.1016/j.neuroimage.2004.07.020.
McIntosh, A.R., Misic, B., 2013. Multivariate statistical analyses for neuroimaging data. In: Fiske, S.T. (Ed.), Annual Review of Psychology vol. 64 (Vol. 64, pp. 499-+).
Misic, B., Fatima, Z., Buschkuehl, M., Churchill, N., Cimprich, B., Deldin, P.J., Berman, M.G., 2014. The functional connectivity landscape of the human brain. PLoS One (in press).
Nolen-Hoeksema, S., Wisco, B.E., Lyubomirsky, S., 2008. Rethinking rumination. Perspect. Psychol. Sci. 3 (5), 400–424. http://dx.doi.org/10.1111/j.1745-6924.2008.00088.x.
Oppenheim, A.V., Schafer, R.W., Buck, J.R., 1999. Discrete-time Signal Processing, 2nd ed. Prentice Hall, Upper Saddle River, NJ.
Raichle, M.E., MacLeod, A.M., Snyder, A.Z., Powers, W.J., Gusnard, D.A., Shulman, G.L., 2001. A default mode of brain function. Proc. Natl. Acad. Sci. U. S. A. 98 (2), 676.
Saad, Z.S., Gotts, S.J., Murphy, K., Chen, G., Jo, H.J., Martin, A., Cox, R.W., 2012. Trouble at rest: how correlation patterns and group differences become distorted after global signal regression. Brain Connectivity 2 (1), 25–32.
Schölvinck, et al., 2010. Neural basis of global resting-state fMRI activity. PNAS 107 (22), 10238–10243.
Sheline, Y.I., Barch, D.M., Price, J.L., Rundle, M.M., Vaishnavi, S.N., Snyder, A.Z., Raichle, M.E., 2009a. The default mode network and self-referential processes in depression. Proc. Natl. Acad. Sci. U. S. A. 106 (6), 1942. http://dx.doi.org/10.1073/pnas.0812686106.
Sheline, Y.I., Barch, D.M., Price, J.L., Rundle, M.M., Vaishnavi, S.N., Snyder, A.Z., Raichle, M.E., 2009b. The default mode network and self-referential processes in depression. Proc. Natl. Acad. Sci. U. S. A. 106 (6), 1942–1947. http://dx.doi.org/10.1073/pnas.0812686106.
Sheline, Y.I., Price, J.L., Yan, Z.Z., Mintun, M.A., 2010. Resting-state functional MRI in depression unmasks increased connectivity between networks via the dorsal nexus. Proc. Natl. Acad. Sci. U. S. A. 107 (24), 11020–11025. http://dx.doi.org/10.1073/pnas.1000446107.
Smith, S.M., Jenkinson, M., Woolrich, M.W., Beckmann, C.F., Behrens, T.E.J., Johansen-Berg, H., Matthews, P.M., 2004. Advances in functional and structural MR image analysis and implementation as FSL. Neuroimage 23, S208. http://dx.doi.org/10.1016/j.neuroimage.2004.07.051 ER.
Smith, S.M., Miller, K.L., Salimi-Khorshidi, G., Webster, M., Beckmann, C.F., Nichols, T.E., Ramsey, J.D., Woolrich, M.W., 2011. Network modelling methods for fMRI. Neuroimage 54, 875–891.
Treynor, W., Gonzalez, R., Nolen-Hoeksema, S., 2003. Rumination reconsidered: a psychometric analysis. Cogn. Ther. Res. 27 (3), 247.
Tzourio-Mazoyer, N., Landeau, B., Papathanassiou, D., Crivello, F., Etard, O., Delcroix, N., Joliot, M., 2002. Automated anatomical labeling of activations in SPM using a macroscopic anatomical parcellation of the MNI MRI single-subject brain. Neuroimage 15 (1), 273–289. http://dx.doi.org/10.1006/nimg.2001.0978.
Veer, I.M., Beckmann, C., Van Tol, M.-J., Ferrarini, L., Milles, J., Veltman, D., Rombouts, S.A.R., 2010. Whole brain resting-state analysis reveals decreased functional connectivity in major depression. Front. Syst. Neurosci. 4. http://dx.doi.org/10.3389/fnsys.2010.00041.
Waites, A.B., Stanislavsky, A., Abbott, D.F., Jackson, G.D., 2005. Effect of prior cognitive state on resting state networks measured with functional connectivity. Hum. Brain Mapp. 24 (1), 59–68. http://dx.doi.org/10.1002/hbm.20069.
Whitfield-Gabrieli, S., Ford, J.M., 2012. Default mode network activity and connectivity in psychopathology. In: NolenHoeksema, S. (Ed.), Annual Review of Clinical Psychology vol. 8. Annual Reviews, Palo Alto (Vol. 8, pp. 49-+).
Williams, J.B., Gibbon, M., First, M.B., Spitzer, R.L., 1992. The Structured Clinical Interview for DSM-III-R (SCID): II. Multisite test–retest reliability. Arch. Gen. Psychiatry 49 (8), 630–636.
Zeng, L.L., Shen, H., Liu, L., Wang, L.B., Li, B.J., Fang, P., Hu, D.W., 2012. Identifying major depression using whole-brain functional connectivity: a multivariate pattern analysis. Brain 135, 1498–1507. http://dx.doi.org/10.1093/brain/aws059.
Zeng, L.-L., et al., 2014. Neurobiological basis of head motion in brain imaging. PNAS 111, 6058–6062.
Zhang, J., Wang, J., Wu, Q., Kuang, W., Huang, X., He, Y., Gong, Q., 2011. Disrupted brain connectivity networks in drug-naive, first-episode major depressive disorder. Biol. Psychiatry 70 (4), 334–342. http://dx.doi.org/10.1016/j.biopsych.2011.05.018.